

COVER PAGE

Document downloaded by @DAEL

Thu Nov 26 19:26:54 2026
For personal use

When automatic English translation is provided, only the original document is authentic.
The EAA cannot be held responsible of any translation error

Bibliographical reference

Optimum Design for Noise Reduction of a Two-Bladed Propeller Fan, Seok-Ho Choi, Kwan-Soo Lee and Jintai Chung, Acta Acustica **vol. 101** (Number 5), 2015, pp. 920-927

DOI
https://doi.org/10.3813/AAA.918887

Acta Acustica united with Acustica
Vol. 101 (2015) 920 – 927

DOI 10.3813/AAA.918887

Optimum Design for Noise Reduction of a Two-Bladed Propeller Fan

Seok-Ho Choi[1)], Kwan-Soo Lee[2)], Jintai Chung[3)]

[1)] Air-conditioning Research Laboratory, LG Electronics Inc., Seoul, 327-23, Korea

[2)] School of Mechanical Engineering, Hanyang University, Seoul, 133-791, Korea. ksleehy@hanyang.ac.kr

[3)] Department of Mechanical Engineering, Hanyang University, Ansan, Kyeonggi-do, 425-791, Korea

Summary

Numerical simulations were performed to investigate the sound generation mechanism of a propeller fan in the outdoor unit of an air conditioner. The vortex and separation flow around two- and three-bladed propeller fans were analyzed to locate the sources of noise. A two-bladed fan usually has a lower flow rate than a three-bladed fan at the same rotating speed. In general, a two-bladed fan should increase the rotating speed to obtain the same amount of flow rate as a three-bladed fan. The increased rotating speed of a two-bladed fan may results in a louder noise comparing a three-bladed fan. To overcome this drawback, an optimized two-bladed fan was proposed by increasing the solidity and pitch angle. During optimizing the two-bladed fan, the relative priorities of the design parameters were evaluated to identify the most important, and these parameters were then optimized using the response surface methodology. The overall sound pressure level (OASPL) of the new optimized two-bladed propeller fan was 5.2 dB lower than that of previous two-bladed fans and 1.2 dB lower than that of the optimized three-bladed fan.

PACS no. 43.28.-g

1. Introduction

Air conditioners are among the most common industrial and home appliances. The global air conditioner market has grown rapidly since 1977, and the inverter air conditioner was introduced in 1982. Manufacturers have recently focused on adding various functions to air conditioners, such as air cleaning, filter cleaning, ventilation, and humidity control. In addition, a great deal of attention has been paid to reducing the noise level in air conditioners, which is generally due to the fan. Air conditioner indoor units contain cross-flow or turbo fans, while shrouded propeller (axial flow) fans are generally used in outdoor units to obtain a high flow rate. Many researchers have studied the performance of propeller fans to maximize their efficiency and flow rate. Considerable efforts have also been made to reduce the noise level through flow field visualization.

Fukano *et al.* [1, 2] performed parametric studies on the propeller fan shroud shape, the distance between the shroud and the rotor leading edge, and the tip clearance. Akaike *et al.* [3] addressed noise reduction of a cooling (propeller) fan for an automobile radiator by optimizing the axial distance between the fan rotor and the shroud using three-dimensional numerical simulations and experimental measurements. Sorensen [4] conducted numerical design optimization to minimize trailing edge noise of rotor-only axial fans. Maaloum *et al.* [5] evaluated the aeroacoustic performance of axial-flow fans using an aeroacoustic approach based on the vortex surface method, and predicted their tonal noise using the Ffowcs Williams–Hawkings (FW-H) equation. In addition, Maaloum *et al.* [6] experimentally analyzed the influence of the upstream environment on the acoustic and aerodynamic behavior of axial fans. Sato and Kinoshita [7] evaluated the performance and studied the noise characteristics of a propeller fan and shroud using an anechoic fan tester and laser Doppler vibrometer. Kamaya and Kanabayashi [8] conducted a parametric study of an axial-flow fan and performed an $L_9(3^4)$ orthogonal array experiment for a small cooling fan to show the effect of each parameter. Fukano *et al.* [9, 10, 11] introduced a very simple physical model that could simulate turbulent noise originating in low-pressure axial-flow fans quite accurately. Jiang *et al.* [12] investigated the noise generation mechanism of a propeller fan in the outdoor unit of an air conditioner, and developed a method for predicting the flow and acoustic pressure field. However, all these studies addressed small axial-flow fans for ventilation and turbines; therefore, there has been little in-depth attention focused on the propeller fan in outdoor units of air conditioners.

Most investigations of propeller fans for air conditioner outdoor units have considered fans with three or more blades. At the same rotating speed, in general, a two-bla-

Received 11 August 2010,
accepted 07 June 2015.

© S. Hirzel Verlag · EAA

ded fan produces a lower flow rate than a three-bladed fan. If increasing the rotating speed of a two-bladed fan to obtain the flow rate of a three-bladed fan, the noise level of a two-bladed fan may become higher than that of a three-bladed fan. To resolve this problem, an improved two-bladed fan with low noise was proposed in this paper, which has the same flow rate and rotating speed as a three-bladed fan. For this purpose, the noise generation mechanism of a two-bladed propeller fan was investigated numerically and a two-bladed fan was optimized. The optimum shape of the proposed two-bladed fan was obtained through an optimization process. The important design parameters of the fan were selected by an orthogonal array experiment, and these parameters were then used to generate the response surface (RS) of the overall sound pressure level (OASPL), which was experimentally measured using an anechoic chamber and a fan tester. Finally the OASPL of the optimized two-bladed fan is compared with that of the optimized three-bladed fan. Because three-bladed fans were studied by many other researchers [12, 13, 14, 15] and this paper was focused on the two-bladed fan, the optimization process of the three-bladed fan is not contained in this paper.

2. Numerical analysis and validation

The standard k–ε model [16] for numerical analysis was used since turbulent flow was anticipated around the fan. The mass, momentum, turbulence energy, and turbulence dissipation rate conservation equations can be expressed by the following equations:

$$\frac{\partial u_i}{\partial x_i} = 0, \tag{1}$$

$$\frac{\partial u_i u_j}{\partial x_j} = -\frac{\partial}{\partial x_i}\left(P + \frac{2}{3}k\right) + \frac{\partial}{\partial x_j}\left[(\nu + \nu_t)\left(\frac{\partial u_i}{\partial x_j} + \frac{\partial u_j}{\partial x_i}\right)\right], \tag{2}$$

$$\frac{\partial k u_j}{\partial x_j} = \frac{\partial}{\partial x_j}\left[\left(\nu + \frac{\nu_t}{\sigma_k}\right)\frac{\partial k}{\partial x_j}\right] + \nu_t S - \varepsilon, \tag{3}$$

$$\frac{\partial \varepsilon u_j}{\partial x_j} = \frac{\partial}{\partial x_j}\left[\left(\nu + \frac{\nu_t}{\sigma_\varepsilon}\right)\frac{\partial \varepsilon}{\partial x_j}\right] + \frac{\varepsilon}{k}\left(C_1 \nu_t S - C_2 \varepsilon\right), \tag{4}$$

where

$$S = \left(\frac{\partial u_i}{\partial x_j} + \frac{\partial u_j}{\partial x_1}\right)\frac{\partial u_i}{\partial x_j}, \quad \sigma_k = 1.0, \quad \sigma_s = 1.3,$$
$$C_1 = 1.44, \quad C_2 = 1.92, \quad C_\mu = 0.09,$$

and $\nu_t = C_\mu k^2/\varepsilon$ [17]. The governing equations given in Equations (1)–(4) were solved using a commercial computational fluid dynamics (CFD) software package, FLUENT. This same software has been widely used in many turbomachinery applications [13, 18, 19]. The nonlinear equations were solved by under- relaxation, and the SIMPLE algorithm [20] was chosen for the pressure–velocity coupling scheme. All discrete scalar equations, including the three momentum equations, were discretized using second-order upwind interpolation. Figure 1 shows the computational domain and the shape of outdoor unit. The grid structure used in this study was the optimum based on the results of many test computations. Because the blade of a propeller fan has complicated curved surfaces, the inner portion of the outdoor unit was modeled by an unstructured tetragonal grid of 4,619,954 cells, and the outer portion of the outdoor unit was modeled by a structured hexagonal grid of 1,263,268 cells. These grids were used to reduce the number of cells in the entire domain. The heat exchanger was considered as a porous media. The sliding mesh method [17] was used to simulate the rotating flow from the propeller fan, and the multiple reference frame (MRF) [17] method was used for the initial conditions.

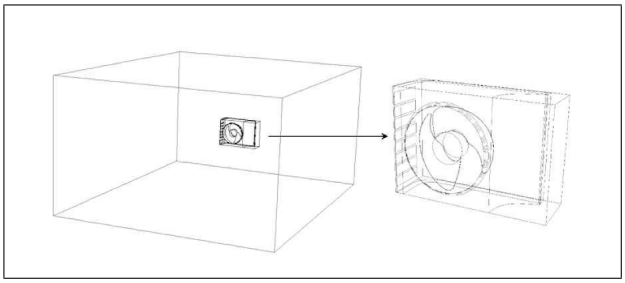

Figure 1. Computational domain. Left: complete domain, right: outdoor unit.

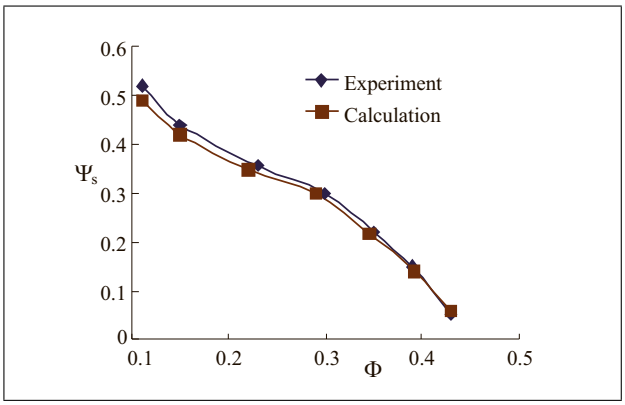

Figure 2. Characteristic curve of the propeller fan.

The numerical results were validated by qualitative and quantitative analyses. Figure 2 shows the characteristic curve of the propeller fan. The numerical and experimental values for the static pressure coefficient $\Phi = 4Q/(\pi^2(D_t^2 - D_h^2)d_t N/60)$ and the flow coefficient $\Psi_s = 2gP_s/(\rho(\pi D_t N/60)^2)$ agreed closely. The fan rotation speed is $N = 700$ rpm and the diameters of the fan tip and hub are $D_t = 400$ mm, $D_h = 135$ mm, respectively. Figure 3 shows the experimental and calculated flow rates of the outdoor unit to demonstrate the validity of the quantitative characteristics. The numerical results were similar to the experimentally measured flow rate with a maximum error of less than 1%.

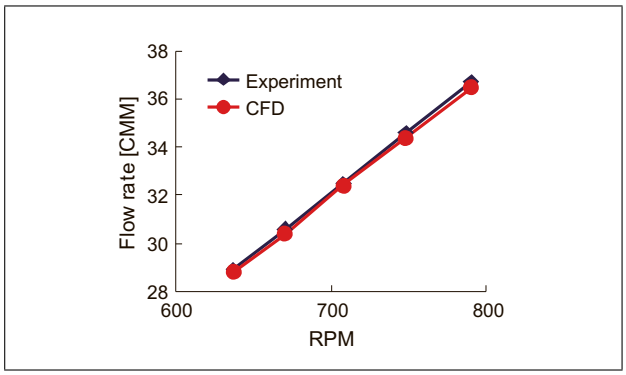

Figure 3. Comparison of the flow rates calculated by CFD and experimentally.

3. Experimental apparatus and procedures

A fan tester was used to measure the flow rate of the outdoor unit, as shown in Figure 4a. The flow rate was determined by measuring the pressure difference between the front and rear of the nozzle with pressure taps and transducers. The signals from the pressure transducers were recorded on a personal computer. The uncertainties of the flow rate measurements were 4.07% calculated from the bias and precision errors of the instruments.

The A-weighted sound pressure level was measured in an anechoic chamber as shown in Figure 4b. The acoustic measurements were based on the ISO 14695:2003 standard (Industrial Fans – Method of Measurement of Fan Vibration). The A-weighted and octave band sound pressure levels were measured using B&K Pulse 3560B and B&K 1/2-inch 4190 microphones. The microphones were calibrated and their measurement consistencies were checked before and after each set of measurements. Other equipment used during the acoustic measurements included a portable tachometer to measure the fan speed, tripods to hold microphones, and a thermometer and barometer to check environmental conditions.

The two microphones for the acoustic measurements were located 1 m in front of and 1 m behind the outdoor unit on the axis of the fan motor, and the outdoor unit was placed on a table 1 m high. The acoustic value was proportional to the noise level of the outdoor unit. The anechoic chamber was 5 m × 5 m× 5 m; the ambient noise level in the chamber was 14.2 dB, and the lowest cutoff frequency was 100 Hz.

4. Flow characteristics of the two-bladed propeller fan

As shown in Figure 5, the two-bladed fan had a larger space between the blades; therefore, it had the advantage of reducing turbulent fluctuation on the blade surface because the flow disturbance between the trailing edge of the preceding blade and the leading edge of the following blade was weaker. Three vortex structures were formed near the propeller fan: the tip vortex, the leading edge separation vortex, and the tip leakage vortex [20, 21]. The tip

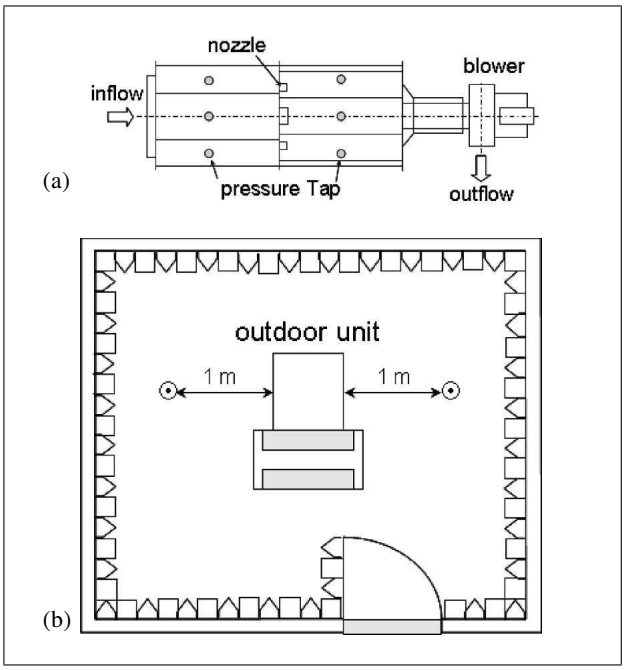

Figure 4. Experimental apparatus showing (a) the fan tester and (b) the anechoic chamber.

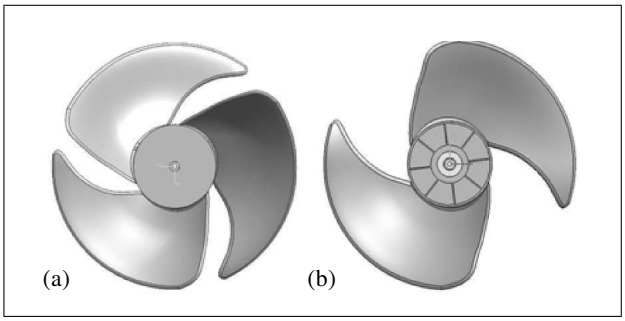

Figure 5. Shape of (a) the three-bladed fan and (b) the two-bladed fan.

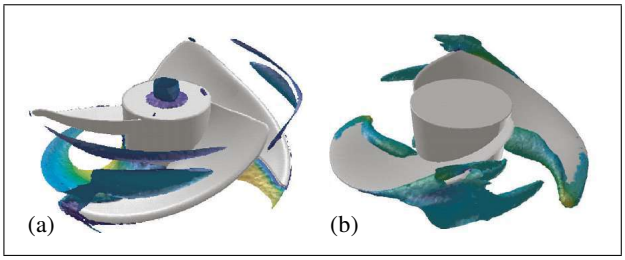

Figure 6. Low-velocity region (less than 1 m/s) around the (a) three-bladed fan and (b) two-bladed fan.

vortex started from the blade tip suction side near mid-chord and impinged on the pressure surface of the adjacent blade. Figure 6 shows a calculated low-velocity region around the propeller fans. All numerical computations in this study were performed with the computational domain, shown in Figure 1, which includes stationary casing and environment. In the two-bladed fan, the tip vortex from the blade tip of the suction side did not reach the pressure surface of the adjacent blade because the distance

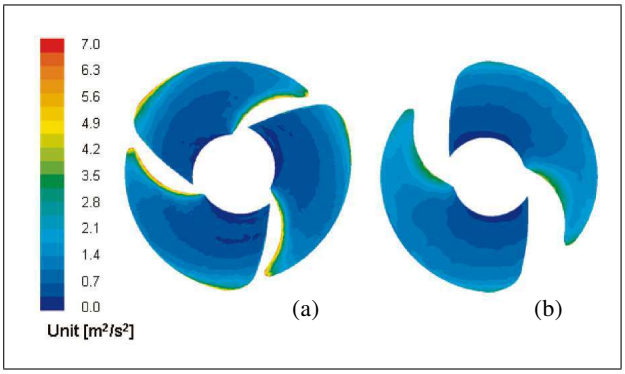

Figure 7. Turbulent kinetic energy distribution on the pressure surface of the blade at 700 rpm for the (a) three-bladed fan and (b) two-bladed fan.

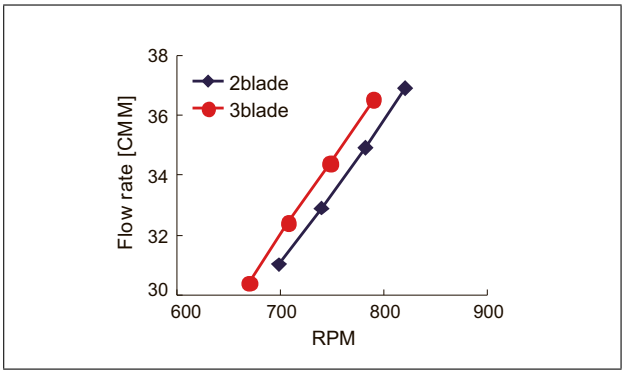

Figure 8. Flow rate for the variation of rotation speed.

between blades was large compared to that of the three-bladed propeller fan.

Figure 7 shows the turbulent kinetic energy distributions on the pressure sides of two- and three-bladed propeller fans for a fan rotation speed of 700 rpm. The two-bladed fan had a lower kinetic energy distribution than the three-bladed fan. The area-averaged kinetic energy of the two-bladed fan was 1.01 m^2/s^2 and that of the three-bladed fan was 1.24 m^2/s^2. Even though the two-bladed fan has the advantage of lower noise, the three-bladed fan is much more commonly used in outdoor unit units of air conditioners because its flow rate is higher for the same rotation speed. Figure 8 shows the relationship between the flow rate and the rotation speed for two- and three- bladed propeller fans. The flow rate of the two-bladed fan was 1.2 m^3/min (CMM) less than that of the three-bladed fan. Increasing the flow rate of the two-bladed propeller fan requires changing the design parameters such as the solidity and pitch angle. The solidity is the ratio of the area of the blade to that of the rotor disc and the pitch angle is the angle between the horizontal plane of rotation of the rotor disc and the chord line of the blade.

Figure 9 shows the static pressure distribution on the blade surface of the two-bladed propeller fan. The static pressure increased gradually from the leading edge, reached a maximum in the middle, and decreased again toward the trailing edge. The pressure drop at the trailing edge induced a separation on the blade surface that re-

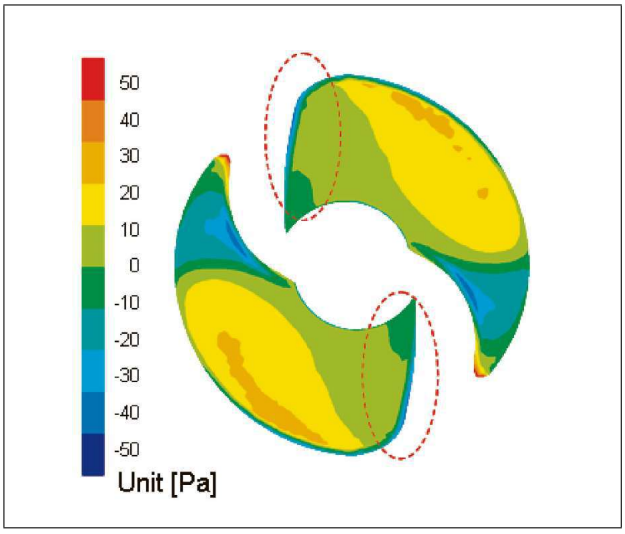

Figure 9. Static pressure distribution on the blade surface of the two-bladed propeller fan.

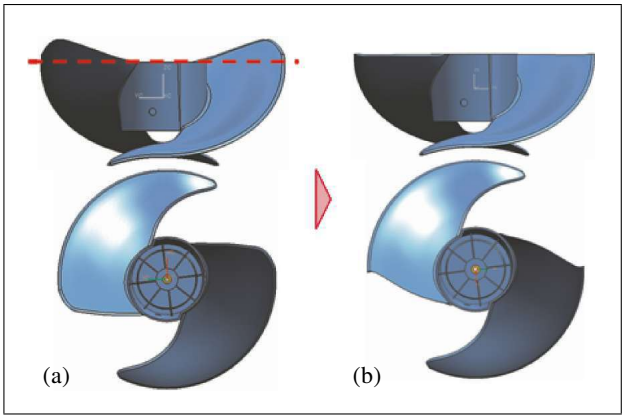

Figure 10. Modification of the blade to increase the pitch angle and solidity without changing the fan height: (a) unmodified base model and (b) modified model.

sulted in a decrease in flow rate. A higher flow rate could be obtained by increasing the solidity and the pitch angle of the fan, although this would increase the fan height. This increased height is generally not acceptable because the depth of the outdoor unit is restricted. Therefore, this paper describes a new type of a propeller fan, the blades of which are trimmed so that they do not extend above the hub. As shown in Figure 10, the fan height was reduced by trimming the useless area of the fan. The solidity and pitch angle could thus be increased without increasing the depth of the outdoor unit. The trimmed blades led to a 5% increase in solidity and a 12% increase in pitch angle compared to the base model. In addition, the noise level was reduced because of the increased space between the trimmed blades. Table I compares the flow rates for three types of propeller fans for a rotation speed of 700 rpm. The modified two-bladed fan model had a 5% greater flow rate than the base two-bladed model and achieved almost the same flow rate as the three-bladed model.

Table I. Comparison of the flow rates for three types of propeller fans for a rotation speed of 700 rpm.

Three-bladed	Two-bladed (base model)	Two-bladed (modified model)
31.9	30.2	31.7

Table II. Orthogonal array of $L_9(3^4)$. α: Pitch angle [°], β: Rake angle [°], γ: Sweep angle [°].

Solidity	α	β	γ	Noise [dB]
0.90	33	25	50	49.2
0.90	35	27	55	48.2
0.90	37	29	60	47.4
0.95	33	27	60	49.2
0.95	35	29	50	48.1
0.95	37	25	55	46.4
1.00	33	29	55	48.2
1.00	35	25	60	47.3
1.00	37	27	50	47.0

Table III. OASPL [dB] for each level of design parameter. α: Pitch angle [°], β: Rake angle [°], γ: Sweep angle [°].

Level	Solidity	α	β	γ
1	48.4	48.9	47.6	48.1
2	47.9	48.0	48.2	47.7
3	47.5	46.9	47.9	48.0
Difference	0.9	2.0	0.6	0.4
Rank	2	1	3	4

5. Orthogonal array experiment

Many parameters affect the flow rate and noise level of propeller fans. Consideration of all the parameters for optimization would require many experiments to generate the appropriate RS. Therefore, parametric studies were conducted to select a small number of vital parameters for optimization. The following were selected as important parameters for the design of experiment methodology: the solidity, pitch angle, sweep angle, and rake angle. An $L_9(3^4)$ orthogonal array was used to investigate the effect of each parameter. This array cannot be used to analyze the interactions among the parameters, but it is capable of illustrating the quadratic effect within the ranges of the parameters. The range of each parameter was limited by the physical geometry of the outdoor unit. The solidity was in the range 0.9–1.0 due to practical manufacturing considerations. The pitch and the rake angles, which were constrained by the depth of the outdoor unit, were in the ranges 33°–37° and 25°–29°, respectively. The sweep angle was in the range 50°–60°, as shown by previous research. Table II gives the $L_9(3^4)$ orthogonal array.

The relative effects of the four parameters used in the parametric study were examined to select the most dominant. Table III lists the OASPL for each level of the four parameters, and also gives the difference between the maximum and minimum OASPL values, and the ranking of the difference. All OASPL in Table III were measured when the flow rate of the fan was 32 CMM. The OASPL difference clearly indicates that the parameters in decreasing order of importance were the pitch angle, solidity, sweep angle, and rake angle. Therefore, the pitch angle and the solidity were selected as the design variables for optimization because they had the most significant effects on the noise characteristics of the propeller fan.

6. Optimization

The optimization to minimize the fan noise was carried out based on the orthogonal array experiments. Many numerical simulation tools are available to predict the noise level of a fan. However, it is not plausible to simulate the noise in detail for a fan with complex geometry. Furthermore, the fan noise emitted by the chassis of an outdoor unit cannot be computed by using the acoustic analogy method of FLUENT. For this reason, an experimental optimization process was performed with the prototype of a real fan.

The two-bladed propeller fan shape was optimized to minimize its OASPL; this required determining the design variables and the objective function. An $L_9(3^4)$ orthogonal array experiment was conducted to select a small number of critical variables. The range of each design parameter was based on the geometric constraints of the outdoor unit. The OASPL was used as the evaluation criterion and evaluated for each set of experimental conditions in the anechoic chamber, where the experimental points were selected using the central composite design (CCD) method [22]. In order to guarantee fair comparisons of OASPL, all the noise levels during the optimization process were measured when the flow rate of the fans was 32 CMM. The RS model for the noise level was created from the experimental results, and a verification test was performed to confirm that the RS model properly represented the true evaluation factors. The augmented Lagrangian method (ALM) [23] was used to find the optimum point in the RS model. Figure 11 shows a flowchart of this optimization process.

The CCD method was used to generate a quadratic OASPL RS, and thirteen experiments were performed. Table IV shows the noise level corresponding to the coded values of the pitch angle and solidity. Figure 12 shows a three-dimensional surface plot of the RS. A quadratic RS was generated using the least-square method from the thirteen sets of experimental data using

$$f(x_1, x_2) = 46.2655 + 0.4333x_1 - 0.1333x_2 + 1.4207x_1^2 + 0.6207x_2^2 + 0.5x_1x_2, \quad (5)$$

Where f is the OASPL RS, x_1 is the coded value of the pitch angle, and x_2 is the coded solidity value. Figure 13 shows the experimental noise levels compared with the values predicted by Equation (5) with a coefficient of determination $R^2 = 0.96$ for the experimental points determined by the CCD method.

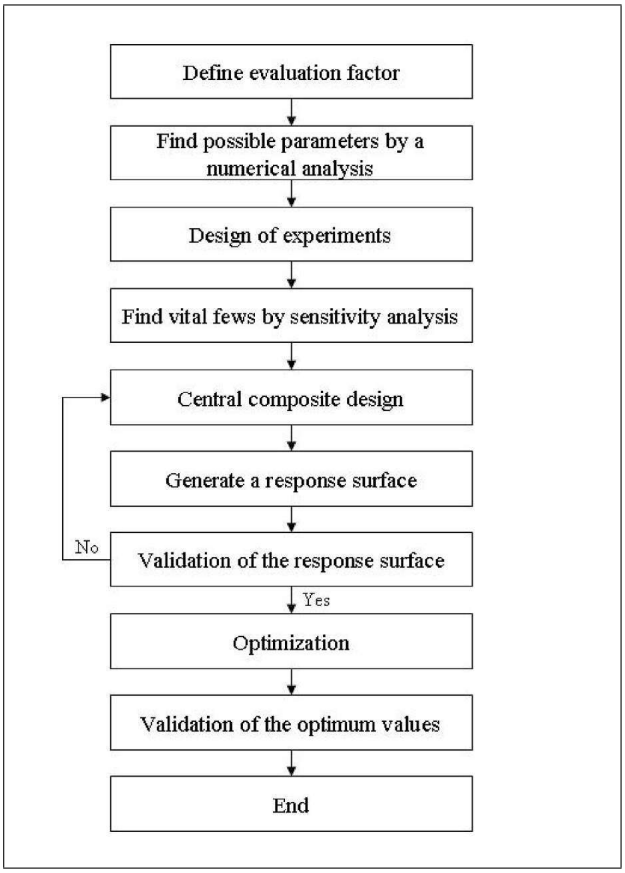

Figure 11. Optimization process flow chart.

Table IV. Design of experiment using the central composite design method.

Run order	Pitch angle x_1	Solidity x_2	Noise [dB]
1	0	−1	47.0
2	−1	1	47.3
3	0	0	46.2
4	0	1	47.0
5	0	0	46.3
6	1	0	48.6
7	1	−1	48.2
8	−1	−1	48.7
9	0	0	46.3
10	−1	0	47.0
11	0	0	46.2
12	0	0	46.1
13	1	1	48.8

Optimization using the RS model was performed by selecting x_1 and x_2 to minimize $f(x_1, x_2)$. The optimum values of the pitch angle and solidity calculated by the ALM were $x_1 = 34.6$ and $x_2 = 0.96$, respectively, resulting in an OASPL of 46.2 dB. Thus, the OASPL for the modified two-bladed propeller fan was reduced by 5.2 and 1.2 dB compared with those for the base two-bladed fan and the optimized three-bladed fan, respectively, when all the fans produced the same flow rate of 32 CMM. Figure 14 shows the sound pressure spectrum of an outdoor unit with the

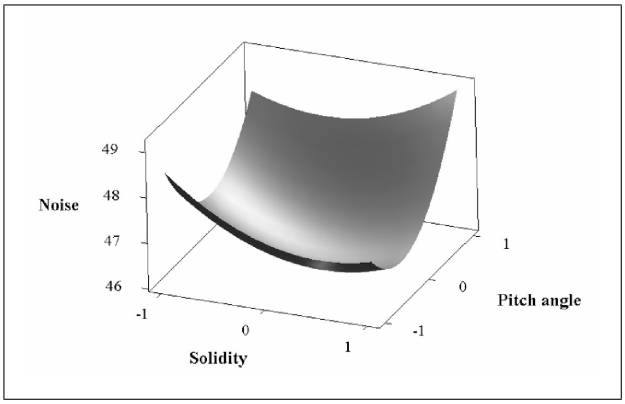

Figure 12. Response surface of the OASPL as a function of solidity and pitch angle.

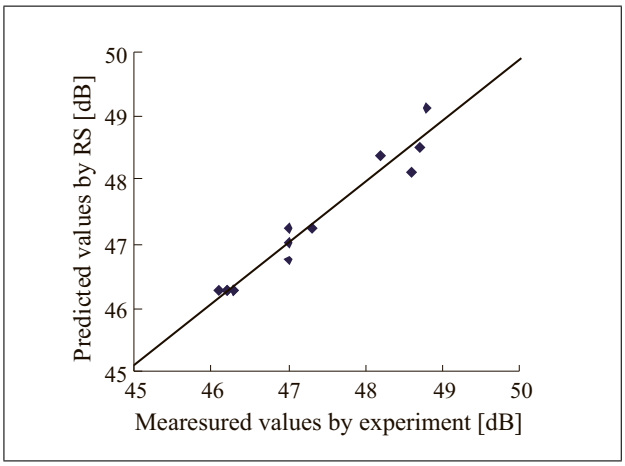

Figure 13. Comparison of the experimentally measured noise values with the computationally predicted noise values.

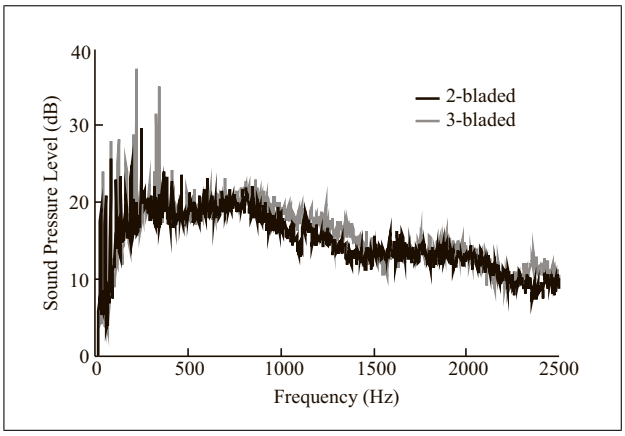

Figure 14. Sound pressure spectra of the outdoor units.

same flow rate of 32 CMM. In order to obtain the same flow rate of 32 CMM, the rotation speeds of the two-bladed and three-bladed fans were adjusted to 824 and 805 RPM, respectively. The optimized two-bladed fan had a lower sound pressure level than the optimized three-bladed fan because the optimization process of the fan shape made the inlet flow of the blades more uniform. In the case of the optimized two-bladed fan, the OASPL between 800 Hz

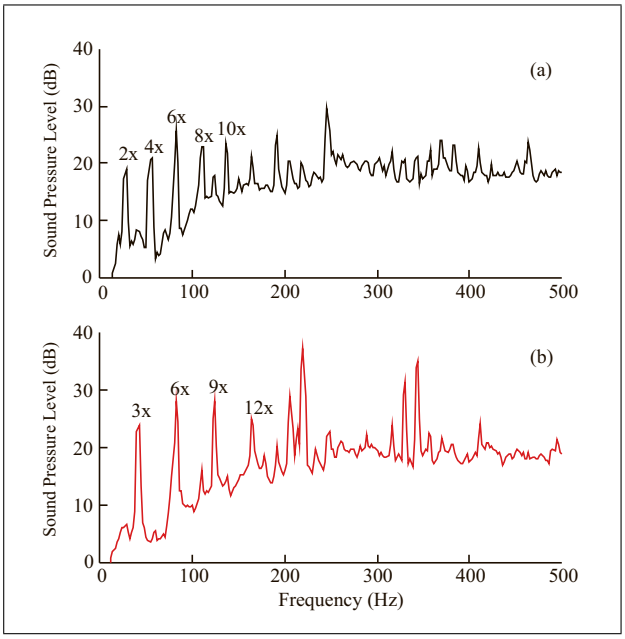

Figure 15. Magnified sound pressure spectra of the outdoor units with (a) the two-blade fan and (b) the three-blade fan.

and 1500 Hz is 40.5 dB and its level is 1.4 dB lower than that of the optimized three-bladed fan. The tip vortex does not impinge on the pressure surface of the adjacent blade in the case of the two-bladed fan. The frequency range of Figure 14 from zero to 500 Hz is magnified in Figure 15. The fundamental frequencies corresponding to the rotation speeds for the two-bladed and three-bladed fans were 13.7 and 13.4 Hz, respectively. Therefore, the blade passing frequencies for the two-bladed and three-bladed fans are 27.4 and 40.2 Hz, which are denoted by 2x and 3x in Figures 15a and 15b. The two-bladed fan has the harmonics of the blade passing frequency e.g., 2x, 4x, 6x and etc., as shown in Figure 15a, while the three-bladed fan has the harmonics 3x, 6x, 9x and etc., as shown in Figure 15b. These noise peaks corresponding to the harmonics are usually associated with the interaction of blade rotation with stationary casing and environment. When comparing Figs 15a and 15b, it can be observed that the two-bladed fan has lower discrete noise than the three-bladed fan. The OASPL from zero to 500Hz is 41.2 dB in the case of the optimized two-bladed fan and its level is 2.3 dB lower than that of the optimized three-bladed fan.

7. Conclusions

A numerical analysis of the propeller fan in the outdoor unit of an air conditioner was conducted. The air flow near the propeller fan was analyzed by CFD and the noise generation mechanism was investigated. Two-bladed propeller fans make less noise and consume less power than three-bladed fans, but they have a lower flow rate than three-bladed fans for the same rotation speed. To overcome this drawback, a new type of two-bladed fan was developed by removing the part of the fan blade where separation occurs. The low flow rate of the two-bladed fan was resolved by increasing the solidity and pitch angle without changing the depth of the outdoor unit. The shape of the proposed two-bladed fan was optimized for the OASPL measured experimentally. In this study, the solidity, pitch angle, sweep angle, and rake angle were selected as important design parameters and it was determined that the pitch angle and solidity had the greatest effect on the OASPL. After optimization, the OASPL of the modified two-bladed propeller fan was 5.2 dB less than that of the base two-bladed fan and 1.2 dB less than that of the optimized three-bladed fan.

References

[1] T. Fukano, M. Fukuhara, K. Kawagoe, Y. Hara, K. Kinoshita: Experimental study on the noise reduction of a propeller fan. 1st report, aerodynamic characteristics (in Japanese). Transactions of the Japan Society of Mechanical Engineers B **56** (1990) 3378–3382.

[2] T. Fukano, M. Fukuhara, K. Kawagoe, Y. Hara, K. Kinoshita: Experimental study on the noise reduction of a propeller fan, 2nd report, noise characteristics (in Japanese). Transactions of the Japan Society of Mechanical Engineers B **56** (1990) 3383–3388.

[3] S. Akaike, S. Kuroki, M. Katagiri: Noise reduction of radiator cooling fan for automobile - Three-dimnesional analysis of the flow between the blades of the fan (in Japanese). Society of Automotive Engineers of Japan **22** (1991) 79–84.

[4] D. N. Sorensen: Mimimizing the trailing edge noise from rotor-only axial fans using design optimization. Journal of Sound and Vibration **247** (2001) 305–323.

[5] A. Maaloum, S. Kouidri, R. Rey: Aeroacoustic performance evaluation of axial flow fans based on the unsteady pressure field on the blade surface. Applied Acoustics **65** (2004) 367–384.

[6] A. Maaloum, S. Kouidri, F. Bakir: Effect of inlet duct contour and lack thereof on the noise generated of an axial flow fan. Applied Acoustics **64** (2003) 999–1010.

[7] S. Sato, K. Kinoshita: Improvement in performance of propeller fans for outdoor units of airconditioners. 4th Asian International Conference of Fluid Machinery, 1993, 166–170.

[8] S. Kamaya, S. Kanabayashi: A study on noise reduction for small axial flow fans. Transactions of the Japan Society of Mechanical Engineers B **56** (1990) 204–208.

[9] T. Fukano, Y. Kodama, Y. Senoo: Noise generated by low pressure axial flow fans. I: Modeling of the turbulence noise. Journal of Sound and Vibration **50** (1977) 63–74.

[10] T. Fukano, Y. Kodama, Y. Senoo: Noise generated by low pressure axial flow fans. II: Effect of number of blade, chordlength and camber of blades. Journal of Sound and Vibration **50** (1977) 75–88.

[11] T. Fukano, Y. Kodama, Y. Senoo: Noise generated by low pressure axial flow fans. III: Effect of rotational frequency, blade thickness and outer blade profile. Journal of Sound and Vibration **56** (1978) 261–277.

[12] C. L. Jiang, J. P. Chen, Z. J. Chen: Experimental and numerical study on aeroacoustic sound of axial flow fan in room air conditioner. Applied Acoustics **68** (2007) 458–472.

[13] X. Zhao, J. Sun, Z. Zhang: Prediction and measurement of axial flow fan aerodynamic and aeroacoustic performance in a split-type air-conditioner outdoor unit. International Journal of Refrigeration **36** (2013) 1098–1108.

[14] Z. Shuiqing, L. Hui, W. Jun: Investigation acoustic effect of the convexity-preserving axial flow fan based on Bezier function. Computers & Fluids **102** (2014) 85–93.

[15] J. Wan-Ho, K. Takashi, K. Takuya, H. Shingo: Study on the CFD method for noise source identification and aeroacoustic analysis of an axial fan. Inter-noise, 2011.

[16] B. E. Launder, N. Shima: Second-moment closure for the near-wall sublayer: Development and application. Journal of Americans for International Aid and Adoption **27** (1989) 1319–1325.

[17] Fluent version 5.0 users manual. Fluent Inc., 1998.

[18] P. J. Hotchkiss, C. J. Meyer, T. W. von Backstrom: Numerical investigation into the effect of cross-flow on the performance of axial flow fans in forced draught air-cooled heat exchangers. Applied Thermal Engineering **26** (2006) 200–208.

[19] M. Ha, S. Heo, C. Cheong, K. Y. Park: Development of new cooling system using nacelle duct. World Academy of Science, Engineering and Technology **61** (2012) 301–304.

[20] S. V. Patankar: Numerical heat transfer and fluid flow. Taylor & Francis, 1980.

[21] C. M. Jang, M. Furukawa, M. Inoue: Analysis of vortical flow field in a propeller fan by LDV measurements and LES. Part 1: Three-dimensional vortical flow structures. Journal of Fluids Engineering-Transactions of the ASME **123** (2001) 748–754.

[22] K. Yang, B. El-Haik: Design for six sigma: a roadmap for product development. McGraw-Hill, 2003.

[23] K. Chung, K. S. Lee, W. S. Kim: Optimization of the design factors for thermal performance of a parallel-flow heat exchanger. International Journal of Heat and Mass Transfer **45** (2002) 4773–4780.